

The **next generation** GBCA  
from Guerbet is here

Explore new possibilities >

Guerbet | 

© Guerbet 2024 GUOB220151-A

# AJNR

## **Hypoattenuation on CT Angiographic Source Images Predicts Risk of Intracerebral Hemorrhage and Outcome after Intra-Arterial Reperfusion Therapy**

Lee H. Schwamm, Eric S. Rosenthal, Clifford J. Swap, Jonathan Rosand, Guy Rordorf, Ferdinando S. Buonanno, Mark G. Vangel, Walter J. Koroshetz and Michael H. Lev

This information is current as of September 27, 2024.

*AJNR Am J Neuroradiol* 2005, 26 (7) 1798-1803  
<http://www.ajnr.org/content/26/7/1798>

# Hypoattenuation on CT Angiographic Source Images Predicts Risk of Intracerebral Hemorrhage and Outcome after Intra-Arterial Reperfusion Therapy

Lee H. Schwamm, Eric S. Rosenthal, Clifford J. Swap, Jonathan Rosand, Guy Rordorf, Ferdinando S. Buonanno, Mark G. Vangel, Walter J. Koroshetz, and Michael H. Lev

**BACKGROUND AND PURPOSE:** Symptomatic hemorrhagic transformation (HT) is a significant complication of intravenous and catheter-based reperfusion. We hypothesized that the degree of vascular insufficiency, reflected as hypoattenuation on initial CT angiography (CTA) axial source images, is predictive of HT risk in stroke patients receiving intra-arterial reperfusion therapy.

**METHODS:** We examined initial CTA source images and follow-up CT scans in 32 consecutive patients. Regions of interest were semiautomatically segmented and reviewed. Mean intensity was determined in the region of maximal hypoattenuation and in normal contralateral tissue, and the arithmetic difference ( $\Delta$ HU) calculated. Receiver operator characteristic (ROC) curves and cross-validation were used to identify threshold  $\Delta$ HU values.

**RESULTS:** Thirteen patients had HT on follow-up CT (seven with parenchymal hematoma, six with hemorrhagic infarction). Patients with and those without HT did not differ in age, blood glucose level, lesion volume, or time to treatment or recanalization, though the former had a greater mean  $\Delta$ HU (9.0 vs 6.3,  $P = .006$ ). The ROC threshold at  $\Delta$ HU  $\geq 8.1$  was 69% sensitive and 90% specific for patients who developed HT (odds ratio = 19.1; 95% confidence interval: 2.9, 125;  $P = .002$ ) and was predictive of poor clinical outcome (modified Rankin scale score  $>2$ ,  $P = .03$ ). Neither HT in general nor parenchymal hematoma subtype was associated with poor outcome.

**CONCLUSION:** The degree of hypoattenuation on initial CTA source images is a risk factor for HT and poor clinical outcome after intra-arterial reperfusion therapy. Prospective validation of this relationship in large populations may permit feasible real-time risk stratification.

Hemorrhagic transformation (HT) can mitigate the benefits of intra-arterial reperfusion therapy involving the use of catheter-based chemical agents (tissue-type plasminogen activator [tPA], platelet glycoprotein inhibitors) or mechanical devices (microcatheters and shaped wires). Although pro-urokinase delivered within 6 hours of stroke onset reduces the incidence of disability in patients with occlusion of the middle cerebral artery stem, hemorrhage rates are increased (1, 2). Although symptomatic HT increases morbidity

and mortality (3–9) and although parenchymal hematoma (PH) may be associated with deterioration, petechial hemorrhagic infarction (HI) may be a marker of early reperfusion in some patients after the intravenous (IV) administration of tPA (4, 10, 11).

There is currently no screening imaging method to predict HT. The volume of nonenhanced CT abnormality is only weakly correlated with clinical outcome after IA thrombolysis (12). Proposed CT predictors of HT after IV tPA therapy are early large territorial ischemic change or hypoattenuation (3, 13–17). Quantification of reductions in the apparent diffusion coefficient on diffusion-weighted MR imaging may help predict hemorrhage (18–22); however, its utility has not been validated in a large series.

The use of CT angiography (CTA) with CT perfusion imaging is a feasible, low-cost method for the evaluation of patients with acute stroke (23–28). With current CT scanners, the neurovascular system from

Received November 24, 2004; accepted after revision January 26, 2005.

From the Departments of Neurology (L.H.S., E.S.R., C.J.S., J.R., G.R., F.S.B., W.J.K.) and Radiology (M.G.V., M.H.L.), Massachusetts General Hospital, Boston, MA.

Author reprint requests to Lee H. Schwamm, Department of Neurology, VBK 915, Massachusetts General Hospital, Boston, MA 02114.

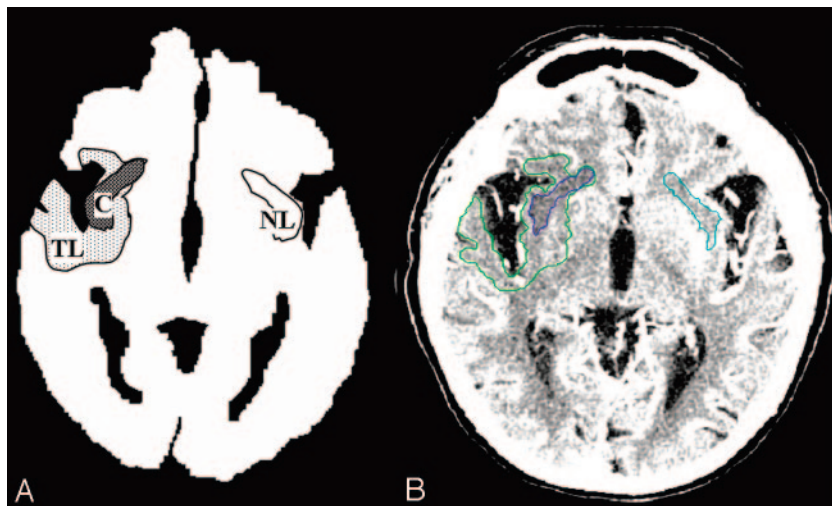


FIG 1. Schematic (A) and contrast-enhanced (B) CTA source images display region-of-interest segmentation. Single-section total lesion volume is the entire region of hypoattenuation on the section containing the core (TL, green). Single-section lesion core is the region of maximal hypoattenuation in the right insula (C, dark blue), compared with normal mirror-image tissue in contralateral left insula (NL, light blue).

the aortic arch to the vertex can be screened within 5 minutes by using a single bolus of contrast material (24–26), and the simultaneously acquired contrast-enhanced axial CTA source images are blood-volume weighted (23, 28). Hypoattenuation on these whole-brain CTA source images is attributable to early ischemic edema and a diminished contrast agent–exchanging blood pool. Results of pilot studies have suggested that hypoattenuation on CTA source images delineates ischemic tissue likely to be irreversibly infarcted and that lesion volume on CTA source images is a stronger predictor of tissue destiny and clinical outcome than the initial scores on the National Institutes of Health Stroke Scale (NIHSS) (28–30).

We sought to determine whether the degree of hypoattenuation on CTA source images is a risk for HT or poor outcome in patients receiving intra-arterial reperfusion therapy for acute occlusion of the middle cerebral or basilar artery.

### Methods

We retrospectively reviewed the clinical and imaging findings of 38 consecutive patients treated with IA reperfusion therapy for proximal occlusion of the middle cerebral or basilar artery within 6 hours of symptom onset. Patients who presented with significant neurologic disability with CTA evidence of middle cerebral or basilar artery occlusion and those in whom the clot could be accessed within 6 hours of symptom onset were selected to receive IA reperfusion therapy. Patients who presented within 3 hours of onset and who were eligible for IV tPA were treated with a 0.09-mg/kg bolus (10% based on a 0.9-mg/kg dose), followed by an IV infusion of tPA until the clot was accessed. Six patients were excluded: four who did not undergo CTA, one who was treated with a laser device, and one who died from vessel rupture during treatment.

NIHSS scores were recorded in the emergency department. All patients received nonenhanced CT, immediately followed by CTA of the circle of Willis and skull base. Synchronous whole-brain perfused blood-volume imaging was performed, as is our routine practice (23). Routine nonenhanced head CT was performed by using a helical CT scanner (High-Speed Advantage; GE Medical Systems, Milwaukee, WI) in the emergency department. This was followed immediately by helical scanning during the administration of 90–120 mL of nonionic

contrast agent (Omnipaque 300, Nycomed Inc./Nycomed AS, Roskilde, Denmark) at 3 mL/s with a 25-second prep delay. All scans were performed with 140 kVp and 170 mAs. Section thickness was 5 mm for nonenhanced scans and 3 mm for CTA source images.

Treatment included IA tPA alone, IA tPA with IV eptifibatid or abciximab ( $n = 17$ ), or IA tPA after a partial dose of IV tPA started within 3 hours of symptom onset (bridging therapy,  $n = 5$ ). A team of experienced interventional neuro-radiologists performed IA reperfusion therapy by using established techniques for tPA infusion and mechanical clot manipulation (31). Patients who had residual thrombus after fibrinolytic therapy or who underwent substantial mechanical clot manipulation also received platelet glycoprotein inhibitors to prevent rethrombosis. Pretreatment and posttreatment arteriograms of the involved vessels were obtained, and the elapsed time between stroke onset and recanalization or procedure termination was recorded.

HT was graded according to the method of European Australasian Acute Stroke Study (17) by means of blinded consensus interpretation of any nonenhanced CT images acquired during the first 8 days of the patient's admission and medical record review. HT was classified according to clinical and radiologic criteria. HI 1 was defined as small petechiae along the margins of the infarct; HI 2, as confluent petechiae in the infarcted area but no space-occupying effect. PH 1 was defined as blood clots in 30% of the infarcted area with some slight space-occupying effect; PH 2, as blood clots in >30% of the infarcted area with a substantial space-occupying effect.

Postprocedural contrast enhancement was differentiated from hemorrhage by means of serial CT examination or, in some cases, MR imaging with susceptibility (32). Intracranial hemorrhage was defined as symptomatic if the patient had clinical deterioration causing an increase in the NIHSS score of  $\geq 4$  and if the hemorrhage was likely to be the cause of his or her clinical deterioration (33). However, when edema or hemorrhage as the leading pathology was in doubt, an association of the hemorrhage with the deterioration was assumed. Clinical outcome was defined by using modified Rankin scale (mRS) scores at 3–6 months after initial presentation, as determined by reviewing the hospital's outpatient stroke database. Our institutional review board approved our retrospective review of all medical and imaging data.

The 3-mm-thick whole-brain CTA source images were evaluated for ischemic regions by identifying areas of relative hypoattenuation. By using a semiautomated software package (Alice; Parexel Corp., Waltham, MA), these ischemic regions of interest were visually segmented (Fig 1) to determine the volume and degree (measured in Hounsfield units) of lesion

**TABLE 1: Characteristics of patients with and without hemorrhagic transformation after IA reperfusion therapy**

	Hemorrhagic Transformation	No Hemorrhagic Transformation	P Value
Patient demographics			
Number of cases	13	19	
Mean age (years)	65.2	67.9	.63
Female (%)	46.2%	52.6%	.99
Clinical characteristics			
Left-hemispheric MCA lesions (%)	33.3%	38.5%	.20
Mean initial NIHSS score	19.9	17.6	.20
Mean initial serum glucose (mg/dl)	186	173	.63
Patients on antithrombotics (%)	53.8%	42.1%	.99
Treatment characteristics			
Mean time from symptoms to initial image (hours)	2.04	1.77	.56
Mean time from symptoms to treatment (hours)	4.33	4.22	.80
Mean time from treatment to recanalization (hours)	0.92	0.95	.92
Patients with recanalization <6 h after onset (%)	69.2%	57.9%	.71
Patients receiving GP-IIb/IIIa inhibitors (%)	54.0%	52.9%	.99
Patients receiving IV tPA (%)	15.4%	15.8%	1.0
Mean dose IA tPA (all patients) (mg)	13.7	10.9	.31
Mean total dose tPA (IV + IA patients) (mg)	24.5	22.9	.87

Note.—GP indicates glycoprotein; IA, intraarterial; IV, intravenous; MCA, middle cerebral artery; NIHSS, National Institutes of Health Stroke Scale; tPA, tissue plasminogen activator.

hypoattenuation. A core lesion was defined as the region of maximal hypoattenuation on a single contrast-enhanced axial section. The mean degree (Hounsfield units) of this lesion was determined. To correct for any within-scan variability, this segmented core was compared with a mirror-image contralateral region of uninvolved tissue (Fig 1). These mirror-image normal regions were matched for gray-white constituents; no CSF spaces, blood vessels, or other volume-averaged tissue were included. Three readers (L.H.S., M.H.L., E.S.R.) who were experienced in the interpretation of stroke CT scans and who were blinded to the patients' clinical histories, lateralization of symptoms, follow-up imaging and clinical outcomes analyzed the images. All imaging studies were independently interpreted during multiple reading sessions by using optimal window width and center level settings to identify subtle differences between normal and hypoattenuating brain parenchyma (34). Disagreements in ratings were resolved by means of consensus blinded review.

A score for the degree of maximal hypoattenuation score ( $\Delta$ HU) was calculated on the section containing the region of maximal hypoattenuation by subtracting the mean HU of the core from the mean HU of the contralateral normal tissue. Compared with findings on the CTA source images, hypoattenuating areas on the admission nonenhanced CT images were typically ill-defined, with indistinct borders. Therefore, segmentation of maximally hypoattenuating regions on nonenhanced CT was achieved only by mapping the segmented regions of interest on the CTA source images to corresponding locations on the non-coregistered, nonenhanced CT images. A post hoc  $\Delta$ HU was then calculated for the nonenhanced CT in the same manner as for the CTA source images.

The resulting  $\Delta$ HU values were compared between patients with and those without HT by using a two-tailed *t* test, the Fisher exact statistic, or the odds ratio (OR) with 95% confidence intervals (CIs), as appropriate. A receiver-operator characteristic (ROC) curve was constructed to determine a  $\Delta$ HU threshold associated with subsequent HT. A cross-validation leave-one-out approach (35) was performed to test the effects of outliers on this threshold. The  $\Delta$ HU value and the presence of HT were also tested for likelihood of poor clinical outcome (mRS > 2), as in the Prolyse in Acute Cerebral Thromboembolism trial (36).

## Results

Thirty-two patients were included in the analysis (Table 1). Thirteen (40%) had evidence of HT on follow-up, and seven had PH. HT was symptomatic in one patient with PH. None had acute pulmonary edema or renal dysfunction due to the contrast agent for CT or conventional angiography, and the scanning procedure did not delay treatment. We found no significant differences between the HT and non-HT groups with regard to relevant clinical and imaging or treatment variables, including timing and/or degree of recanalization. The main finding was that patients with HT had a mean  $\Delta$ HU on CTA source images greater than that of patients without HT (9.0 vs 6.3,  $P = .006$ ). However, mean  $\Delta$ HU values were not significantly different for patients with HT and PH versus those with HT but not PH (9.0 vs 6.9,  $P = .14$ ) (Table 2).

The ROC curve for  $\Delta$ HU demonstrated that the operating point of  $\Delta$ HU >8.1 had 69% sensitivity and 89% specificity for predicting HT after IA therapy (OR = 19.1; 95% CI: 2.9, 125;  $P = .002$ , Fisher exact statistic) (Fig 2). Application of this threshold produced two false-positive and four false-negative predictions of HT, the smallest total error in predicting HT for any single threshold (Fig 1). Cross-validation to test for the effect of outliers resulted in seven false-positive or false-negative results (22%), compared with six errors (19%) under the ROC curve-derived threshold. This finding confirmed that no single data point overly influenced the prediction mode. (The optimal threshold remained at  $\Delta$ HU >8.1 for 31 of 32 omissions and  $\Delta$ HU >7.9 for one of 32 omissions.) The area under the ROC curve for the accuracy of predicting hemorrhage by using CTA source images was 81% compared with 76% ( $P = .54$ )

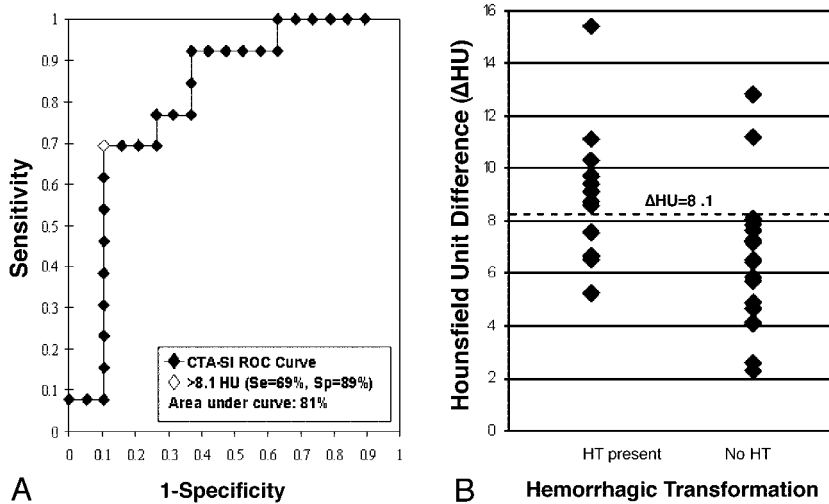


FIG 2. Relationship between  $\Delta$ HU of the lesion core and the likelihood of hemorrhage after IA reperfusion therapy. A, ROC curve from which an optimal  $\Delta$ HU threshold was selected. B, Scatterplot of patients with or without HT after IA reperfusion therapy.

TABLE 2: Imaging findings in patients with and without hemorrhagic transformation after IA reperfusion therapy

	Hemorrhagic Transformation	No Hemorrhagic Transformation	P Value
CTA-SI (prospective segmentation)			
Total lesion volume (ml)	51.5	30.8	.20
Single slice lesion volume on slice containing core (ml)	2.5	2.0	.46
Core lesion volume (ml)	0.24	0.32	.06
Single slice lesion mean $\Delta$ HU (HU) (normal tissue HU - single slice lesion HU on single slice containing core)	3.6	3.2	.63
Core Mean $\Delta$ HU (HU) (normal tissue HU - core lesion HU)	9.0	6.3	.006
Unenhanced CT (post hoc segmentation)			
Single slice lesion mean $\Delta$ HU (normal tissue HU - single slice lesion HU on single slice containing core) (HU)	5.8	3.3	.02

Note.—CT indicates computed tomography; CTA-SI, computed tomography angiography source images;  $\Delta$ HU, Hounsfield units.

derived for nonenhanced CT images segmented on the basis of the CTA source images.

A  $\Delta$ HU value of  $>8.1$  on admission CTA source images was also predictive of poor clinical outcome at 3–6 months. Patients with  $\Delta$ HU  $>8.1$  were more likely than those with  $\Delta$ HU  $\leq 8.1$  to have an mRS score of  $>2$  at follow-up (82% vs 38%; OR = 7.3; 95% CI: 1.2, 42.8;  $P = .03$ , Fisher exact statistic). The presence of HT in the poor outcome group did not entirely account for this association. Although poor outcomes were more common in patients with HT than in those without HT (69% vs 42%; OR = 3.1; 95% CI: 0.7, 13.7;  $P = .17$ , Fisher exact statistic), and in those with PH compared with those without PH (71% vs 48%; OR = 2.7; 95% CI: 0.4, 16.7;  $P = .40$ , Fisher exact statistic), these trends were not statistically significant.

Nonenhanced CT images analyzed after the CTA source images in post hoc fashion showed a similar relationship, though the  $\Delta$ HU value was objectively less conspicuous. On nonenhanced CT images, mean  $\Delta$ HU was greater in patients with HT than in patients without HT (5.8 vs 3.3,  $P = .02$ ) (Table 2). The ROC curve for  $\Delta$ HU constructed from the post hoc segmented nonenhanced CT images revealed that, at an operating point of  $\Delta$ HU  $>3.8$ , sensitivity was 85% and specificity was 68% for identifying patients who

developed HT after IA therapy. However, for this dataset, these values were not statistically significant (OR = 2.8; 95% CI: 0.7, 11.6;  $P = .29$ ). In a paired  $t$  test, CTA source images generated greater lesion conspicuity (ie,  $\Delta$ HU) than the nonenhanced CT images in all patients (7.4 vs 4.3,  $P < .00001$ ) and in the subgroup who subsequently developed HT (9.0 vs 5.8,  $P = .0006$ ).

### Discussion

Identifying predictors of HT may improve the selection of patients for reperfusion therapy. Although predictors of HT on nonenhanced CT after IV tPA treatment have been described (3, 13–17, 36, 37), little is known about predictors of HT after IA reperfusion therapy. Focal hypoattenuation on CTA source images may reflect a profound degree of ischemia-induced endothelial injury with increased risk of reperfusion hemorrhage (18) or inadequate leptomeningeal collateral blood flow (26, 28, 38). Our data suggested that axial source images are readily acquired and that they provide a visually detectable threshold of hypoattenuation without postprocessing that is a powerful independent predictor of both HT and poor outcome after IA reperfusion. The ROC-

curve threshold remained robust under a cross-validation analysis, even in this small cohort.

Regions of abnormality on the nonenhanced CT usually cannot be segmented prospectively because of their ill-defined borders; areas of abnormality are more conspicuous on CTA source images. Previous data from coregistered subtraction analyses suggest that, among patients treated with IA reperfusion therapy, a large fraction of CTA hypoattenuation in the 3–6-hour range is due to change in cerebral blood volume and not tissue attenuation visible on nonenhanced CT alone (39). This increased conspicuity can improve the accuracy of localizing ischemia compared with the accuracy of reviewing nonenhanced CT scans (40). For the group developing HT, regions of hypoattenuation on CTA source images were 55% more conspicuous (by mean  $\Delta$ HU) than on the corresponding initial nonenhanced CT images; likewise, the derived prediction threshold was 113% more conspicuous. The small threshold of  $\Delta$ HU >3.8 determined on post hoc analysis of nonenhanced CT images offered one reason why regions of hypoattenuation on nonenhanced CT could not be segmented until CTA source images were viewed. At the low-contrast detectability of current CT scanners (image noise standard deviations of about 0.3%–0.5%, or 3–5 HU) (41), small differences may not be visually appreciated on nonenhanced CT.

More than 20 years ago, investigators recognized that delayed CT after a high-dose infusion of iodinated contrast agent can depict early breakdown of the blood-brain barrier in patients with acute stroke and normal nonenhanced CT scans who presented within 28 hours of symptom onset. Patients with this finding were at high risk for HI and thought to be unsuitable candidates for surgical reperfusion therapy or systemic anticoagulation (42). Ischemic regions that were invisible on scans obtained with their early-generation CT scanners are likely to be evident on images acquired with today's high-resolution scanners and reviewed by adjusting the window width and center level to display the full DICOM dataset (34). However, the authors demonstrated that they could heighten the sensitivity of conventional CT by using iodinated contrast agent and thus identify patients at increased risk of brain hemorrhage with reperfusion therapies. In this sense, Hayman et al were pioneers who blazed a similar trail to ours more than 2 decades ago (42).

Our study had several limitations. For instance, the method of semiautomated image segmentation by means of visual inspection may have been subject to bias. Scans suggestive of a poor prognosis for reasons other than hypodensity such as presence of tumor may potentially be segmented differently or given increased attention. To anticipate these concerns, segmentation was performed in a blinded manner, and all regions were verified by consensus. In addition, all CTA source images were analyzed before the nonenhanced CT scans were reviewed. Furthermore, our cohort might not have been large enough to demonstrate that PH is a significant risk factor for

poor clinical outcome or to detect other potential confounders, given the low frequency of symptomatic HT. Findings in this cohort of patients treated with IA reperfusion therapy could not validate the observation that HI in patients treated with IV thrombolysis may be a marker of early reperfusion (11). In addition, the use of mechanical clot manipulation and, in some patients, the use of IV tPA before or platelet glycoprotein inhibitors after IA tPA may have introduced unaccounted for variability. Because the number of these patients is small, the lack of any subgroup differences may reflect type I error rather than a true lack of effect. Last, many scans were obtained longer than 3 hours after symptom onset, and whether the hypoattenuation threshold determined from this dataset is generalizable to CT scans obtained within 3 hours after symptom onset or to cohorts receiving different patterns of subacute care is unclear. Further studies in a dataset larger than ours are needed to verify whether the relationship between hypoattenuation on CTA source images and HT persists after investigators adjust for these factors in a formal logistic regression.

## Conclusion

Notwithstanding these limitations, detecting an 8 HU difference between a region of maximal hypoattenuation on CTA source images and the contralateral normal tissue is straightforward and easily applied at the CT scanner or a low-cost image workstation. This difference may help in identifying patients who are at increased risk of hemorrhage or poor clinical outcome after intra-arterial reperfusion therapy.

## References

1. del Zoppo GJ, Higashida RT, Furlan AJ, Pessin MS, Rowley HA, Gent M. **PROACT: a phase II randomized trial of recombinant pro-urokinase by direct arterial delivery in acute middle cerebral artery stroke—PROACT investigators.** *Prolyse in acute cerebral thromboembolism.* *Stroke* 1998;29:4–11
2. Furlan A, Higashida R, Wechsler L, et al. **Intra-arterial prourokinase for acute ischemic stroke: the PROACT II study—a randomized controlled trial.** *Prolyse in acute cerebral thromboembolism.* *JAMA* 1999;282:2003–2011
3. NINDS t-PA Stroke Study Group. **Intracerebral hemorrhage after intravenous t-PA therapy for ischemic stroke.** *Stroke* 1997;28:2109–2118
4. Larrue V, von Kummer R, del Zoppo G, Bluhmki E. **Hemorrhagic transformation in acute ischemic stroke. Potential contributing factors in the European Cooperative Acute Stroke Study.** *Stroke* 1997;28:957–960
5. Motto C, Ciccone A, Aritzu E, et al. **Hemorrhage after an acute ischemic stroke: MAST-I collaborative group.** *Stroke* 1999;30:761–764
6. Jaillard A, Cornu C, Durieux A, et al. **Hemorrhagic transformation in acute ischemic stroke: the MAST-E study.** *Stroke* 1999;30:1326–1332
7. Multicenter Acute Stroke Trial—Europe Study Group. **Thrombolytic therapy with streptokinase in acute ischemic stroke.** *N Engl J Med.* 1996;335:145–150
8. Hacke W, Kaste M, Fieschi C, et al. **Intravenous thrombolysis with recombinant tissue plasminogen activator for acute hemispheric stroke: the European Cooperative Acute Stroke Study (ECASS).** *JAMA* 1995;274:1017–1025
9. Hacke W, Kaste M, Fieschi C, et al. **Randomised double-blind**

- placebo-controlled trial of thrombolytic therapy with intravenous alteplase in acute ischaemic stroke (ECASS II). Second European Australasian Acute Stroke Study investigators. *Lancet* 1998;352:1245-1251
10. Berger C, Fiorelli M, Steiner T, et al. Hemorrhagic transformation of ischemic brain tissue: asymptomatic or symptomatic? *Stroke* 2001;32:1330-1335
  11. Molina CA, Alvarez-Sabin J, Montaner J, et al. Thrombolysis-related hemorrhagic infarction: a marker of early reperfusion, reduced infarct size, and improved outcome in patients with proximal middle cerebral artery occlusion. *Stroke*. 2002;33:1551-1556
  12. Roberts HC, Dillon WP, Furlan AJ, et al. Computed tomographic findings in patients undergoing intra-arterial thrombolysis for acute ischemic stroke due to middle cerebral artery occlusion: results from the PROACT II trial. *Stroke* 2002;33:1557-1565
  13. Dubey N, Bakshi R, Wasay M, Dmochowski J. Early computed tomography hypodensity predicts hemorrhage after intravenous tissue plasminogen activator in acute ischemic stroke. *J Neuroimaging* 2001;11:184-188
  14. Tanne D, Kasner SE, Demchuk AM, et al. Markers of increased risk of intracerebral hemorrhage after intravenous recombinant tissue plasminogen activator therapy for acute ischemic stroke in clinical practice: the Multicenter rt-PA Stroke Survey. *Circulation* 2002;105:1679-1685
  15. von Kummer R, Allen KL, Holle R, et al. Acute stroke: usefulness of early CT findings before thrombolytic therapy. *Radiology* 1997;205:327-333
  16. Molina CA, Montaner J, Abilleira S, et al. Timing of spontaneous recanalization and risk of hemorrhagic transformation in acute cardioembolic stroke. *Stroke* 2001;32:1079-1084
  17. Larrue V, von Kummer RR, Muller A, Bluhmki E. Risk factors for severe hemorrhagic transformation in ischemic stroke patients treated with recombinant tissue plasminogen activator: A secondary analysis of the European Australasian Acute Stroke Study (ECASS II). *Stroke* 2001;32:438-441
  18. Knight RA, Barker PB, Fagan SC, Li Y, Jacobs MA, Welch KM. Prediction of impending hemorrhagic transformation in ischemic stroke using magnetic resonance imaging in rats. *Stroke* 1998;29:144-151
  19. Adami A, Thijs V, Tong DC, Beaulieu C, Moseley ME, Yenari MA. Use of diffusion weighted MRI to predict the occurrence and severity of hemorrhagic transformation in a rabbit model of embolic stroke. *Brain Res* 2002;944:32-39
  20. Tong DC, Adami A, Moseley ME, Marks MP. Relationship between apparent diffusion coefficient and subsequent hemorrhagic transformation following acute ischemic stroke. *Stroke* 2000;31:2378-2384
  21. Tong DC, Adami A, Moseley ME, Marks MP. Prediction of hemorrhagic transformation following acute stroke: role of diffusion- and perfusion-weighted magnetic resonance imaging. *Arch Neurol* 2001;58:587-593
  22. Selim M, Fink JN, Kumar S, et al. Predictors of hemorrhagic transformation after intravenous recombinant tissue plasminogen activator: prognostic value of the initial apparent diffusion coefficient and diffusion-weighted lesion volume. *Stroke* 2002;33:2047-2052
  23. Hunter GJ, Hamberg LM, Ponzio JA, et al. Assessment of cerebral perfusion and arterial anatomy in hyperacute stroke with three-dimensional functional CT: early clinical results. *AJNR Am J Neuroradiol* 1998;19:29-37
  24. Lev MH, Farkas J, Rodriguez VR, et al. CT angiography in the rapid triage of patients with hyperacute stroke to intraarterial thrombolysis: accuracy in the detection of large vessel thrombus. *J Comput Assist Tomogr* 2001;25:520-528
  25. Knauth M, von Kummer R, Jansen O, Hahnel S, Dorfler A, Sartor K. Potential of CT angiography in acute ischemic stroke. *AJNR Am J Neuroradiol* 1997;18:1001-1010
  26. Wildermuth S, Knauth M, Brandt T, Winter R, Sartor K, Hacke W. Role of CT angiography in patient selection for thrombolytic therapy in acute hemispheric stroke. *Stroke* 1998;29:935-938
  27. Klotz E, Konig M. Perfusion measurements of the brain: using dynamic CT for the quantitative assessment of cerebral ischemia in acute stroke. *Eur J Radiol* 1999;30:170-184
  28. Lev MH, Segal AZ, Farkas J, et al. Utility of perfusion-weighted CT imaging in acute middle cerebral artery stroke treated with intra-arterial thrombolysis: prediction of final infarct volume and clinical outcome. *Stroke* 2001;32:2021-2028
  29. Schramm P, Schellinger PD, Fiebich JB, et al. Comparison of CT and CT angiography source images with diffusion-weighted imaging in patients with acute stroke within 6 hours after onset. *Stroke* 2002;33:2426-2432
  30. Berzin TM, Lev MH, Goodman D, et al. CT perfusion imaging versus MR diffusion weighted imaging: prediction of final infarct size in hyperacute stroke. *Stroke* 2001;32:317
  31. Budzik R, Pergolizzi R, Putman C. Intraarterial thrombolysis for acute ischemic stroke. *Semin Neurosurg* 2000;11:107-132
  32. Greer DA, Koroshetz WJ, Cullen S, Gonzalez RG, and Lev MH. Magnetic resonance imaging improves detection of intracerebral hemorrhage over computed tomography after intra-arterial thrombolysis. *Stroke* 2004;35:491-495
  33. National Institute of Neurological Disorders and Stroke rt-PA Stroke Study Group. Tissue plasminogen activator for acute ischemic stroke. *N Engl J Med* 1995;333:1581-1587
  34. Lev MH, Farkas J, Gemmete JJ, et al. Acute stroke: improved nonenhanced CT detection—benefits of soft-copy interpretation by using variable window width and center level settings. *Radiology* 1999;213:150-155
  35. Efron B, Tibshirani RJ. *An Introduction to the Bootstrap*. New York: Chapman and Hall; 1993
  36. Wechsler LR, Roberts R, Furlan AJ, et al, for the PROACT II investigators. Factors influencing outcome and treatment effect in PROACT II. *Stroke* 2003;34:1224-1229
  37. Gilligan AK, Markus R, Read S, et al. Baseline blood pressure but not early computed tomography changes predicts major hemorrhage after streptokinase in acute ischemic stroke. *Stroke* 2002;33:2236-2242
  38. Lee KH, Cho SJ, Byun HS, et al. Triphasic perfusion computed tomography in acute middle cerebral artery stroke: a correlation with angiographic findings. *Arch Neurol* 2000;57:990-999
  39. Bove P, Lev MH, Chaves T, et al. CT perfusion imaging of hyperacute stroke: subtraction analysis of infarct conspicuity. Oak Brook, IL: American Society of Neuroradiology. *Proceedings of the 39th Annual Meeting of the American Society of Neuroradiology*. 2001.
  40. Ezzeddine MA, Lev MH, McDonald CT, et al. CT angiography with whole brain perfused blood volume imaging: added clinical value in the assessment of acute stroke. *Stroke* 2002;33:959-966
  41. Haaga JR, Alfidi RJ. *Computed Tomography of the Whole Body*. Washington, DC: C. V. Mosby; 1988
  42. Hayman LA, Evans RA, Bastion FO, Hinck VC. Delayed high dose contrast CT: identifying patients at risk of massive hemorrhagic infarction. *AJR Am J Roentgenol* 1981;136:1151-1159